



Tailings Dam's Safety Assessment Considering Undrained Foundation Failure

Flávia Augusta Padovani¹ and Thiago Bretas²(✉)

¹ BVP Geotecnia e Hidrotecnicia, Belo Horizonte, MG, Brazil

² TBretas Consultoria, Belo Horizonte, MG, Brazil

tbretas@tbretas.com

Abstract. During construction and raising phases of tailings dams, excess pore pressures and localized deformations (plasticization zones) may develop due to applied overloads. Therefore, it can develop an undrained shearing in contractile materials, as tailings and foundation soils. In this case, the design of these structures must consider, in its studies, the failure by undrained shearing of the foundation as a potential trigger for static liquefaction of tailings. In Brazil, National Mining Agency - Resolution No. 13 set a minimum safety factor equal to 1.3 for stability analyzes and studies of liquefaction susceptibility considering peak undrained shear strength. In this context, the present work aims to present the safety assessment of a hypothetical tailing dam, for an undrained scenario (which was considered even for the foundation), in view of the main consolidated methodologies in the geotechnical community, for shear resistance parameters estimation. The stability analyses were developed in 2-D and 3-D, by limit equilibrium method. The results indicated overestimated factors of safety when considering effective strength parameters for the foundation, reinforcing the importance of carefully evaluating the type of mechanical behavior of soils under shearing.

1 Introduction

During construction or tailings facilities raising phases, loading applications, excess pore pressures development, water level raise and local strains may trigger static liquefaction on some materials, as pore pressure raises and consequently, effective tailings shear strength lows.

From historical cases of liquefaction collapses, like Los Frailes Dam and Mount Polley Dam, it was observed that tailings liquefaction may be triggered by foundation failure in cohesive soils, with low excess pore pressure drainage capacity (low permeability). Los Frailes tailings facility in Spain, a rockfill dam, even downstream raised, collapsed in 1998 triggered by strength loss of foundation, in highest cross-section, where there was 60 cm thick layer of marine clay under a 4m thick layer of alluvium (Alonso and Gens 2006).

The gold Tailings dam, in Mount Polley mine, in turn, collapsed in 2014 due to undrained behavior of a foundation “glaciolacustrine” superficial layer (Vick et al. 2015).

Given these events and knowing that loading imposed on contractive materials may trigger high excess pore pressures, the use of undrained shear strength parameters is more suitable to assess tailings facilities **stability** built over cohesive soils, with low

drainage rates during collapse. Stability assesses using effective shear strength may lead to unreal factor of safety, even if consider high water levels and conservative effective parameters such as cohesion and friction angle (Ladd 1991).

In case of center line raised tailings dam, this failure mode is even more critical because part of dam's body is supported on generally loose, saturated and unconsolidated tailings.

Therefore, to reach reliable factor of safeties, it is crucial to adopt adequate shear strength parameters that represents mechanical behavior of dam's materials.

2 Contractive Behavior Tendency Under Shear

The stability analysis on Figure 1a, represents a embankment tailings dam, center line raised. The foundation is a residual soil superficial layer over altered rock.

The behaviors of both residual soil and tailings, under shear, were assessed through lab tests results such as CIUsat and CPTu's field tests (cone penetration test with pore pressure measurement).

The contractive potential of the reservoir's tailings was verified using CPTu tip resistance results (q_c), sleeve friction (f_s) and porewater pressure (u_2), by Robertson (2016) methodology. Data processing was carried out according to Soil Behavior Type (Mod. SBTn), proposed by Robertson (2016), which representation is through Qtn Graph (dimensionless normalized tip resistance) versus Fr (normalized sleeve friction).

According to the Mod. SBTn proposed by Robertson (2016), those tailings presents predominantly contractive behavior, once the majority of the points lie below $CD=70$ line, suggesting behavior equivalent to sensitive clays (CCS). Points distribution on QTN vs Fr graph is presented on Figure 2. CPTu tests profiles are indicated on Figure 3. Due to the general homogeneity/isotropy observed throughout the tailings deposit, it can be said that they are typical profiles.

The State Parameter (ψ) was also evaluated, according to Been and Jefferies (1985), which refers, by definition, to the difference between the initial void ratio *in situ* condition (e) with the void ratio in the critical state (e_c). Materials with a tendency to contract during shear have ψ greater than -0.05 . The red line presented in the graph of ' ψ vs depth', Figure 3, represents the limit of contractive – dilatant behaviors, that is, $\psi = -0.05$. Based on this evaluation, there was a tendency to shrink and, therefore, the extremely loose condition the tailings are in (ψ_{mean} equal to 0.3).

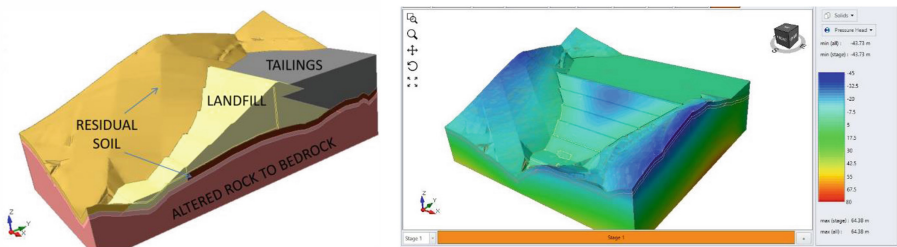


Fig. 1. Numerical modelling 1a) Cross-Section 1b) 3D Seepage analysis – RS3

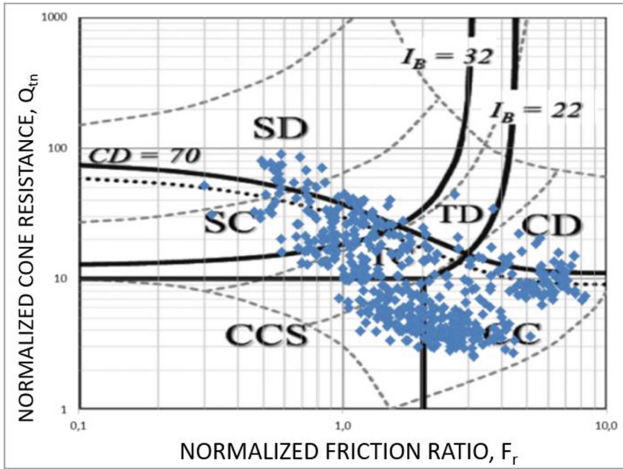


Fig. 2. Qtn vs Fr Graph (Robertson 2016)

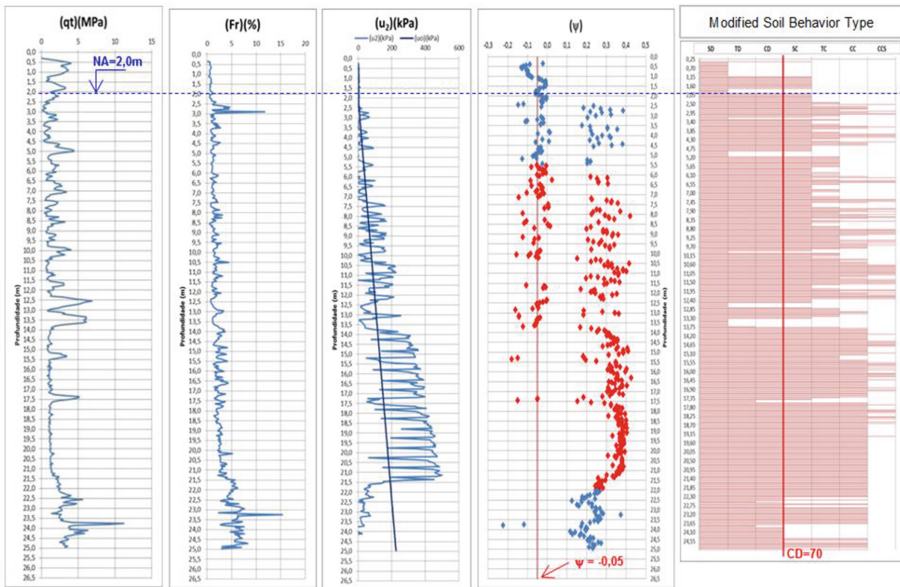


Fig. 3. Typical tailings profile according to CPTu tests (Robertson 2016)

For the foundation residual soil, on the other hand, the results of CIU_{sat} tests were evaluated in terms of deviatoric stress (σ_d), axial deformation (ϵ_a) and excess pore pressure (Δu). The pore pressures were constantly increasing throughout the shear test phase, showing a clear tendency of material contraction during the shear process under undrained conditions, as represented in the path p' ($=\sigma_1 + \sigma_3 / 2$) vs q ($=\sigma_1 - \sigma_3 / 2$) (Fig. 5).

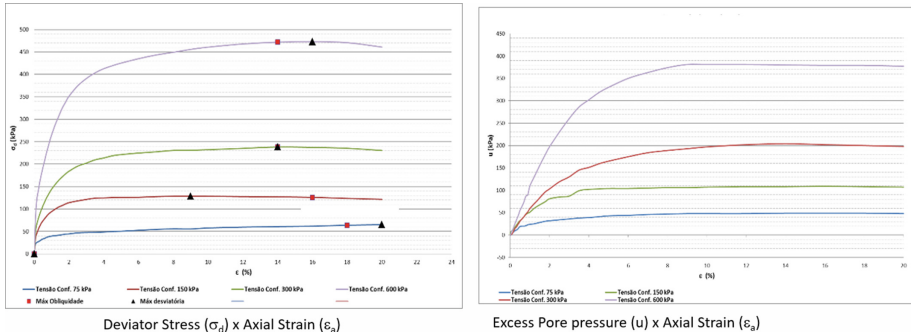


Fig. 4. CIUsat results – residual soil

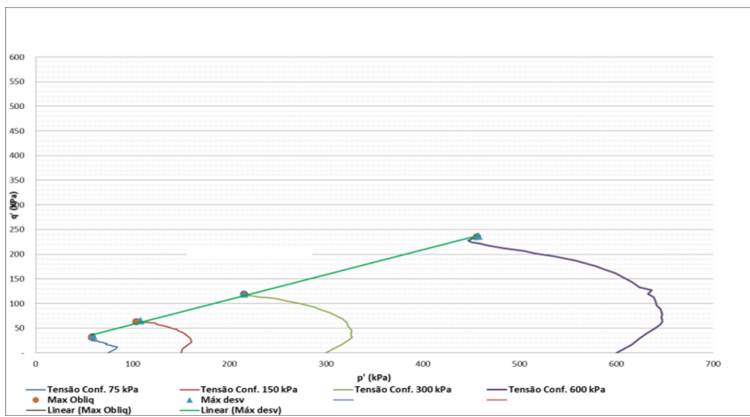


Fig. 5. Effective Stress Paths – p' vs q – residual soil

3 Undrained Shear Strength Parameters Estimation

For the reservoir tailings, the estimate of peak undrained strength ratio ($S_u(\text{PICO}) / \sigma'v$) was determined from the values of tip resistance (q_c), sleeve friction (f_s) and porewater pressure (u_2) measured by CPTu test (Figure 3), according to Olson and Stark (2003) empirical correlations. It is worth mentioning that this formulation is only applicable to materials layers with corrected tip resistance, q_{c1} , lower than 6.5 MPa.

For the peak shear strength, the calculated frequency distribution (histogram) per layer was evaluated, being considered as representative those that correspond to the 20-30% percentile. The adopted criteria is consistent with the 20th percentile suggested by Jefferies & Been (2015). The results distribution histogram is shown in Figure 6, based on the undrained strength ratio ($S_u(\text{PICO}) / \sigma'v$) equal to 0.20 for the tailings, referring to the 25th percentile.

Regarding to foundation residual soil, the peak undrained strength ratio was obtained from Direct Simple Shear (DSS) tests performed on undisturbed samples, at constant volume. This condition is guaranteed using rings around the specimen, which restrict any lateral deformations. In addition, the specimen height is kept constant by varying the

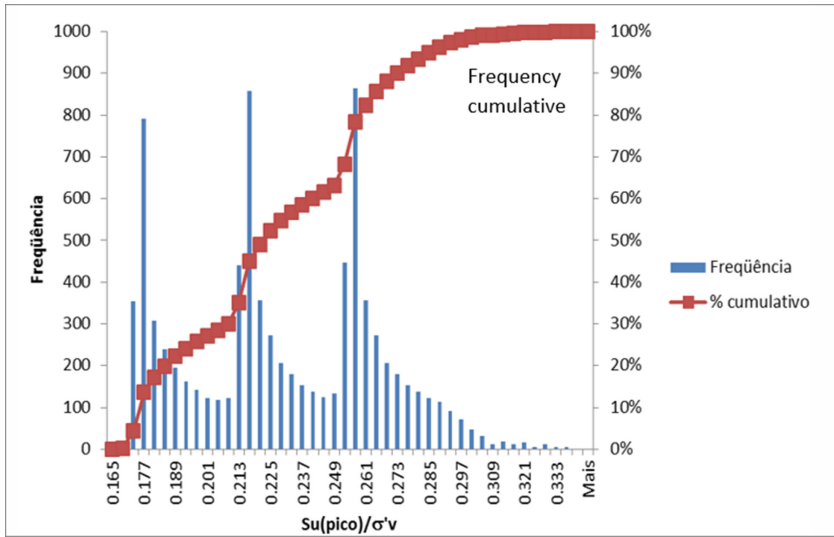


Fig. 6. Undrained peak shear ratio histogram (Olson and Stark 2003)

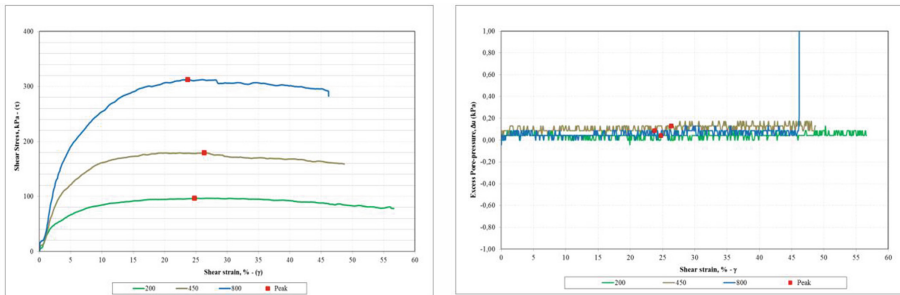


Fig. 7. a) shear stress (τ) vs shear strain (γ); e b) excess pore pressure (u) vs shear strain (γ)

vertical load on the sample, that is, by increasing the load when the specimen is dilated or by relieving it in cases where the soil tends to contract.

Therefore, although drainage is allowed during the test, due the vertical stress and volume are kept constant, the vertical stress variation applied to the specimen is equivalent to the excess pore pressure generated during a truly undrained test (Fronza 2017).

Figure 7 presents the the DSS tests results on residual soil for confining stresses of 200kPa, 450kPa and 800kPa, in terms of shear stress and excess pore-pressure developed during the shear phase. Note that the soil did not show a significant loss of post-peak strength, a mechanical behavior consistent with CIUsat triaxial tests results (Fig. 4). Considering the point of maximum shear stress of the tests performed, the ratio $Su(PEAK)/\sigma'v$ equal to 0.35 for residual soil was obtained (Figure 8).

Additionally, the residual soil undrained strength (Su) was evaluated through its correlation with the NSPT index, inferred from percussion soundings carried out in situ, according to Terzaghi and Peck (1967). To know:

$$Su \text{ (kPa)} = 6 \times NSPT \tag{1}$$

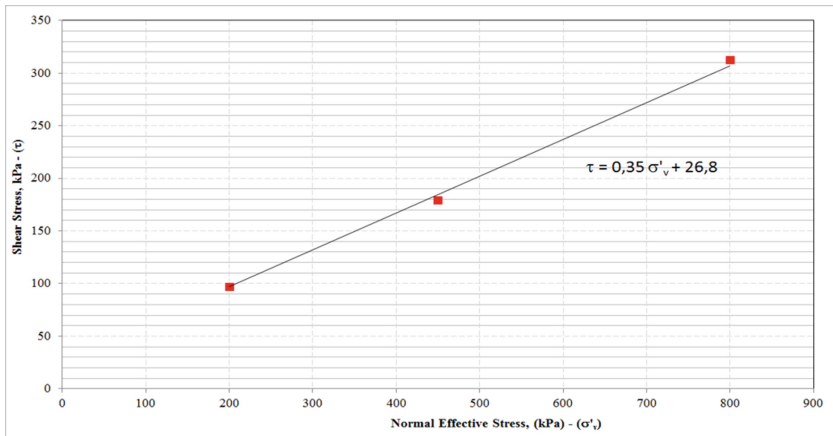


Fig. 8. Shear Stress (τ) x Normal Effective Stress (σ'_v)

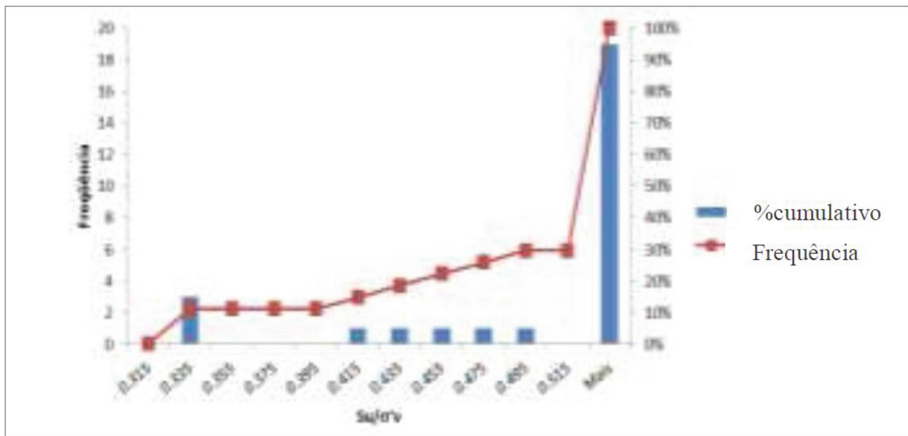


Fig. 9. $S_u(\text{Peak})/\sigma'_v$ Histogram (according to Terzaghi and Peck 1967)

For the residual soil, it was obtained by the Eq. 1 S_u/σ'_v equal to 0.40, considering as selection criterion values referring to the 25th percentile of the frequency distribution histogram (Fig. 9).

Such methodology was considered for purposes of comparison with the shear parameter indicated by the DSS tests. In situations of insufficient or non-existence of laboratory tests, the use of the correlation suggested by Terzaghi and Peck (1967) may be more relevant. Therefore, for the stability analysis, a peak undrained strength ratio equal to 0.34 was adopted for the residual soil, according to laboratory tests results.

4 Results

For stability studies, the strength and specific weight parameters summarized in Table 1 were adopted, with emphasis on those attributed to residual soil and tailings whose interpretation was discussed in the present work.

The three-dimensional numerical model was developed with AutoCad Civil 3D software, from Autodesk, where the surfaces of natural terrain, geomechanical and geological contacts, downstream and upstream slopes and tailings reservoir were created. To define the water table, a 3D seepage analysis was carried out using RS3 software (Rocscience), whose results are shown in Fig. 1b. The 3D stability analysis were carried out using Rocscience Slide3, which calculates the safety factor by limit equilibrium method, considering that surface is discretized in columns, with a square cross section.

Two-dimensional stability analysis were performed on cross-sections traced on the 3D model, using the sections defined as most critical by 3D numerical studies. For the stability analysis, Rocscience Slide2 was used, considering non-circular surfaces search, since circular surfaces are based on relatively simple shapes. In cases of lower strength layers or contacts, preferential failure planes may occur in these regions, conditioning irregular failure surfaces (Duncan 2015). After performing the calculations using the “Cuckoo Search” search algorithm and the rigorous GLE/Morgenstern-Price method, the critical failure surface, shown in Fig. 10, was obtained.

Table 1. Shear strength and permeability parameters

Material	γ	c'	ϕ'	$Su_{(YIELD)}/\sigma'v$	k	kv/kh
	(kN/m^3)	(kPa)	($^\circ$)		(m/s)	
Landfill	19	15	31	-	$1,3 \times 10^{-5}$	0,25
Residual Soil	16	21	30	0,35	$2,0 \times 10^{-5}$	1,00
Altered Rock - Bedrock	16	36	34	-	$1,4 \times 10^{-5}$	1,00
Drain	19	0	30	-	$1,0 \times 10^{-2}$	1,00
Tailing	19	0	25	0,20	$1,0 \times 10^{-4}$	1,00

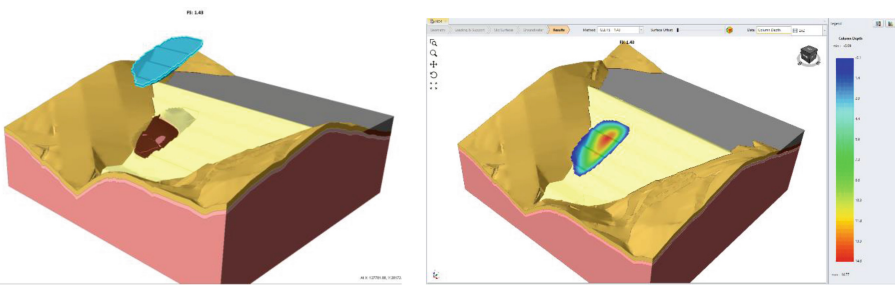


Fig. 10. 3D stability analysis – residual soil with undrained shear strength - FS = 1.43 a) critical failure surface; b) column depth (max = 15m)

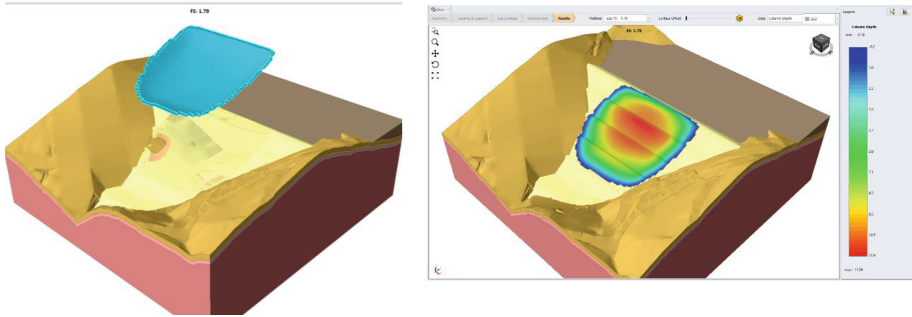


Fig. 11. 3D stability analysis – residual soil with effective shear strength - FS = 1.79 a) critical failure surface; b) column depth (max = 12m)

If a detailed evaluation of foundation behavior under shear was not carried out, that is, if effective shear strength were adopted for residual soil, it would be obtained a overestimated factor of safety, according to the results shown in Fig. 11.

5 Conclusions

From the results obtained by both 2D and 3D analysis carried out in this work, it was possible to conclude that the factor of safety (FS) obtained are satisfactory regarding the criteria recommended by ANM Resolution No. 13 (ANM 2019 – Brazilian Nacional Mining Agency), which fixed FS_{minimum} greater than or equal to 1.3 for the peak undrained condition. The evaluation of natural residual soil behavior under undrained shear should be considered by tailings facilities safety assessments since foundation failure can trigger tailings liquefaction. In this sense, historical cases of Los Frailes Dam and Mount Polley Dam can be mentioned.

The significant difference of factor of safety considering undrained vs drained foundation parameters can be explained through the schematic representation of stress paths presented by Sladen et al. (1985). According to Sladen et al. (1985), materials with a contraction tendency under shear present undrained paths 1–2–3 (undrained strength analysis – USA). In a drained shear condition, these same materials present path 1–4 (effective stress analysis - ESA), which eventually reaches a higher envelope, therefore, with parameters higher than those obtained by the undrained path (trajectory 1–2–3).

The factor of safety obtained also demonstrate that the 2D analysis tend to be more conservative, with FS values lower than the 3D analysis. According to Bretas (2020) the difference in the safety factors of 2D and 3D analyzes can be up to 30% .

The difference in values observed for the FS can be explained by the fact that in 3D stability analysis, the effect of confinement provided by the abutments is considered. In 2D analysis there are limitations, as it is assumed that the failure surface occurs in a plane with infinite extension and, therefore, disregards the effect of shear resistance at the end of the surface (Fredlund et. al. Fredlund et al. 2017).

References

- Agência Nacional de Mineração (2019): ANM. Resolution nº 13, de 8 de agosto de 2019. (2019)
- Alonso, E. E.: Gens, A. Aznalcóllar dam failure. Part 1: Field observations and material properties, v. 56(3), p. 165–183, *Canadian Géotechnique Journal* (2006).
- Been, K., Jefferies, M.G.: A state parameter for sands, v. 35(2), p. 99–112, *Géotechnique*, ICE Virtual Library (1985).
- Been, K., Jefferies, M.G.: *Soil liquefaction: a critical state approach*, 2nd ed., CCR Press. (2015).
- Bretas, T.C.: *Retroanálise Probabilística Tridimensional de taludes em Belo Horizonte*. Master Thesis. NUGEO / UFOP (2020).
- Duncan, J.M., Wright, S.G., Brandon, T.L.: *Soil Strength and Slope Stability*, 2nd ed., John Wiley & Sons, New York, NY, USA (2015).
- Fredlund, M.D.; Fredlund, D. G., Zhang, L.: Moving from 2D to a 3D unsaturated slope stability analysis. In: *PanAm Unsaturated Soils* (2017).
- Fronza, F.: *Análise do comportamento de um solo argiloso marinho em ensaios de cisalhamento simples (DSS) cíclico*. Master Thesis. COPPE. UFRJ (2017).
- Ladd, C.C.: Stability evaluation during staged construction. In: *Journal of Geotechnical Engineering*. ASCE library, v. 117, April, p. 537–615. (1991).
- Olson, S.M.; Stark, T.D.: Yield strength ratio and liquefaction analysis of slopes and embankments. In: *Journal of Geotechnical and Geoenvironmental Engineering*, ASCE library, v. 129(8), p. 727–737. (2003).
- Robertson, P. K.: Cone penetration test (CPT)-based soil behavior type (SBT) classification system — an update. In: *Canadian Geotechnical Journal*. v. 00. (2016)
- Sladen, J.A.; D'Hollander; R.D.; J. Krahn: The liquefaction of sands, a collapse surface approach. In: *Canadian Geotechnical Journal*, v. 22, p. 564–578. (1985).
- Terzaghi, K.; Peck, R. B.; Mesri, G.: *Soil Mechanics in Engineering Practice*, 3rd ed., John Wiley & Sons, New York, NY, USA. (1967)
- Vick, S.; Morgenstern, N.; Zyl, D.V. (2015). Report on Mount Polley Tailings Storage Facility Breach: Independent Expert Engineering Investigation and Review Panel Report. (2015). Available: <<https://www.mountpolleyre.com/viewpanel.ca/final-report>>. Last accessed in 06 mar. 2020.

Open Access This chapter is licensed under the terms of the Creative Commons Attribution-NonCommercial 4.0 International License (<http://creativecommons.org/licenses/by-nc/4.0/>), which permits any noncommercial use, sharing, adaptation, distribution and reproduction in any medium or format, as long as you give appropriate credit to the original author(s) and the source, provide a link to the Creative Commons license and indicate if changes were made.

The images or other third party material in this chapter are included in the chapter's Creative Commons license, unless indicated otherwise in a credit line to the material. If material is not included in the chapter's Creative Commons license and your intended use is not permitted by statutory regulation or exceeds the permitted use, you will need to obtain permission directly from the copyright holder.

